POLITECNICO DI TORINO
Repository ISTITUZIONALE

Integrated receivers with bottom subcooling for automotive air conditioning: detailed experimental study of their filling capacity

(Article begins on next page)

25 April 2024

INTEGRATED RECEIVERS WITH BOTTOM SUBCOOLING FOR AUTOMOTIVE AIR CONDITIONING: DETAILED EXPERIMENTAL STUDY OF THEIR FILLING CAPACITY

F. Cola**,+, M. De Gennaro**, D. Perocchio*, E. Canuto*, S. Daniele*, P. Napoli*, G. Toscano Rivalta*, E. Chiavazzo**, M. Fasano**, P. Asinari**,++

** Department of Energy, Politecnico di Torino, Turin - 10129, Italy

*DENSO Thermal Systems / Technical European Centre, Poirino - 10046, Italy

+School of Mechanical & Aerospace Engineering, Nanyang Technological University, Singapore

++Corresponding author, Tel: +39-011-0904434, Fax: +39-011-0904499,

pietro.asinari@polito.it

ABSTRACT

The use of the integrated receiver in condensers for common automotive air conditioning - A/C - systems is widespread, because of its thermodynamic and operational advantages. Many studies have been already conducted on estimating the effect of the subcooling value. However, this study aims at determining the most important factors affecting the length of the refrigerant stable operating plateau and how the receiver filling is affected by geometrical and thermodynamic boundary conditions, by means of an experimental campaign built using design of experiments - DOE - techniques. Results demonstrate how the receiver diameter and the axle spacing between its inlet and outlet holes have the highest influence on the receiver operation. Finally, these results have been used to set up a numerical model able to accurately estimate the filling efficiency of the integrated receiver, in terms of volume of the operating plateau compared to the net available receiver volume.

Keywords: Automotive air conditioning, condenser, integrated receiver, efficiency

NOMENCLATURE

D	diameter of the receiver (m)
ε	efficiency (-)
h	height of the volume from the receiver base (m)
hv	net height of the volume from the receiver base without plug (m)
ΔH	distance between inlet and outlet holes (m)
V	volume (m^3)

1. INTRODUCTION

The integrated receiver (Fig. 1a – 1b) made its first appearance in the '90s, as an improvement of the parallel flow condenser with flat tubes and multiple louvered fins (Fig. 2), which represents the state-of-art of modern technology in this field, according to Shah [1]. Many studies aimed at optimizing the louver performance, such as the one of Ferrero et. al [2] and Jang and Cheng [3], other focused their attention on the integrated receiver use.

Yamanaka [4] and Burk [5] proved the many advantages of this technology; they discovered that, from a thermodynamic point of view, the receiver ensured a more stable operation of the refrigerant cycle: this is because, by imposing a certain degree of subcooling, a refrigerant flow with liquid phase only could enter the expansion valve, thus reducing the operation instabilities of this component. As a result, a flow with lower vapour quality could enter the evaporator, enhancing its cooling performance.

Other assets of this technology found by Yamanaka, Burk and later by Pomme [6], involve costs and weight savings, and most importantly refrigerant saving; in particular Yamanaka demonstrated that the use of an integrated receiver could save around 150 g of refrigerant, which was previously added in order to force the subcooling and reduce the vapour quality of the flow. Qi et al. [7] studied an air conditioning system that uses microchannels heat exchangers and an integrated receiver condenser. A condenser weight and volume reduction of about 15 % was estimated, with respect to standard condensers; furthermore, refrigerant saving of 50 g was measured.

Studies were conducted aiming at optimizing the operation of both the separate and the integrated receiver condensers, focusing in particular on the role of subcooling; a good review of the various stategies to provide subcooling in vapor compression systems is brought by Qureshi and Zubair [8], though here we will concentrate mainly on subcooling strategies for automotive applications. Khan and Zubair [9], while addressing the improvement offered by mechanical subcooling in separate receiver condenser, proposed a model capable of estimating its optimal value; results showed that such value is related to the saturation temperature of the subcooler used, whose optimal value is about halfway between condensation and evaporation temperatures. Lee and Yoo [10], instead of using a subcooler, studied optimal performance in relation with refrigerant charge; an overcharge of 10% was found to be the best operating condition for the whole air conditioning system. Vyacheslav et al. [11] also studied the effect of the refrigerant charge. A mathematical model was then proposed, which can determine the value of charge that maximizes the COP: results of the simulation were in good accordance to the experimental data. Pomme [12]

also demonstrated the influence of the subcooling value on the COP of the refrigerant cycle; in particular, it was found out that an optimal subcooling value exists, which maximizes the COP. The use of an integrated receiver then can provide the necessary geometrical boundary conditions in order to have the desired degree of subcooling. This is also the first study particularly focusing on the magnitude of the operating plateau: Pomme in fact claims that this value is influenced by the internal volume of the receiver and its capacity in separating the refrigerant gaseous and liquid phases. Jensen and Skogestad [13] estimated that imposing a certain degree of subcooling, by means of a control valve, energy savings in the compressor work up to 2% are achievable, though there are some concerns about the efficacy of such control strategy. Koeln and Alleyne [14] studied a similar control strategy; they confirmed the existence of an optimal subcooling value, which changes according to operating conditions; an extreme seeking control strategy that acts on the control valve was then proposed, and results showed a 9% increase in efficiency of the A/C system.

Further investigations on the receiver were performed by Parrino et al. [15], who conducted a detailed study about the effect of the its volume on the refrigerant optimal charge and the A/C system performance. These Authors demonstrated that in a well-balanced A/C system the receiver capacity yields a small effect on the efficiency of operation, but if the system is not well-balanced, a reduction of the receiver capacity causes stability problems.

The capacity of phase separation was investigated by Prolss et al. [16]. In this study a transparent receiver was used to analyze how good the separation is, using refrigerant charge steps of 100g each. It was demonstrated that the degree of separation influences the liquid stored in the receiver, and it exists, for the integrated receiver, an interval of specific charge where the COP has the maximum value, which represents the operating plateau of the receiver.

Strupp [17] made a similar test on a transparent receiver, again with large refrigerant charge steps, and confirmed the existence of an optimal subcooling value that maximizes the COP. Similar results were obtained by Pottker [18].

The studies made so far yielded an analysis of the subcooling effect on the COP of the A/C cycle; although some studies made an effort to focus on the receiver operating plateau, a thorough investigation is still missing. In addition, studies on the refrigerant optimal charge were done using large charge steps, which may not give enough information on mid and small scale phenomena.

This study gives a higher level of detail on the analysis of the refrigerant optimal charge and on the magnitude of the operating plateau, aiming at maximizing the latter, and subsequently at a cost reduction and refrigerant saving by the enhancement of the receiver filling efficiency.
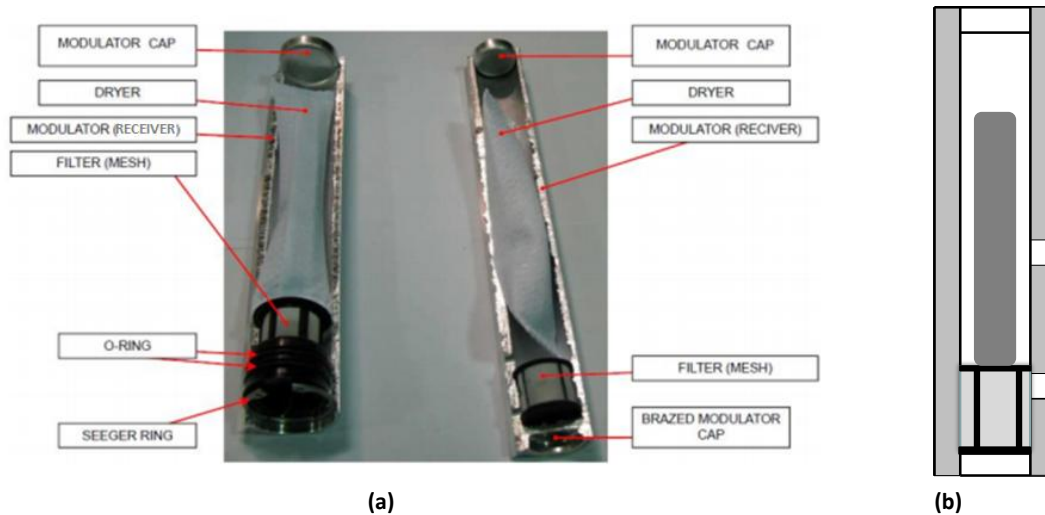
Figure 1. Cross section of a receiver: (a) main features and (b) receiver scheme
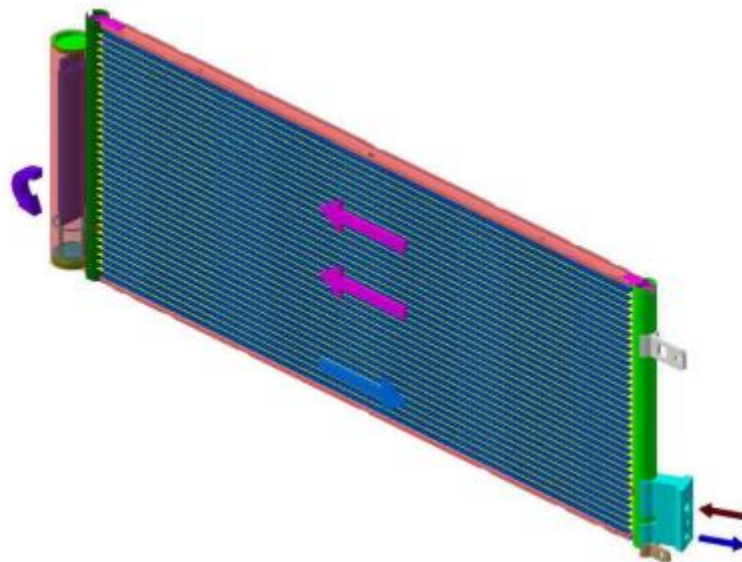

Figure 2. Two-passages parallel flow condenser with integrated receiver

This paper is organized as follows. In section 2 the test bench is presented, along with a description of its set up procedures. In section 3, starting hypothesis and the methodology used to plan the experimental campaign are described. In section 4, results of the test on the transparent receiver are summarized and discussed. In section 5, results of the experimental campaign are provided. Finally, in section 6, the construction of the filling efficiency model is presented. Finally, conclusions are drawn in section 7.

2. SYSTEM TEST BENCH

2.1. Description and instruments set up

The experimental campaign has been conducted using an industrial system test bench which is capable to reproduce similar operating conditions as in vehicle tests.

The system consists of the four basic components of a standard refrigeration cycle: a piston compressor with variable stroke, the expansion valve, condenser and evaporator. The latter two elements are installed in two separate wind tunnels with controllable air flow rate (by means of a fan and a calibrated orifice that measure the current flow rate value) and temperature (via electrical resistors placed at the fan exit that can be operated from the control panel of the test bench). Additionally, in the evaporator wind tunnel, regulation of air relative humidity is possible by two water boilers and a dry compressed air injector.

Other sensors are also present for the measurement of temperature and pressure of the refrigerant fluid at the inlet and outlet of the four main components of the cycle.

The refrigerant R134a is injected by means of a new charge system able to produce charge steps of 5g each with precision of +/- 2g; this system allows the realization of optimal charge tests with a new level of detail never achieved before, making it possible to highlight mid and small scale phenomena that may affect the magnitude of the operating plateau.

In this machine, an electrovalve is located downstream of the charging tube, while in commercial machines electrovalves are usually placed upstream. The electrovalve located downstream allows to keep the charging tube always full of liquid refrigerant, avoiding its weight fluctuations and, for this reason, ensuring stability in measurement.

Setup operations of all the mentioned instrumentation were carried out. In particular, the accuracy of the air flow rate measurement in the two wind tunnels was assessed with tests using a calibrated hole and a hot wire anemometer, following the calibration standard UNI EN ISO 5167-1; the accuracy measured is +/- 2% of the instantenous value measured. For pressure measurement of the refrigerant Model DRUCK Series PTX 500 sensors were used, with accuracy of 0.7% of the fullscale, while air pressure measurement was obtained using Model FUJI Series FCX sensors, with accuracy of +/- 0.3% of the instantaneous value. Temperatures were measured using type T rigid thermocouples for the refrigerant, with +/-0.3 °C accuracy, and type T wire thermocouple for air, with +/- 0.5 °C accuracy. Finally, refrigerant mass flow was measured using a Endress & Hauser PROMASS 83 sensor, with accuracy of +/- 0.1% of the instantaneous value for mass flows between 10% and 100% of the maximum mass flow allowed, and +/- 0.5% under 10% of the istantaneous value.

2.2 Preliminary tests

Five preliminary tests were carried out using a commercial condenser, in order to find a set of standard operating conditions to be used during the entire experimental campaign (Table 1). These tests were performed acting on the air flow rate and the inlet air temperature in the wind tunnels, on the relative humidity in the evaporator wind tunnel and on the compressor velocity. Using different values for these parameters, several optimal charge tests were performed aiming at obtaining the most stable operating conditions, which result in a stable operating plateau.

	Set up	A	B	C	D	E
Working conditions	Condenser Inlet Temp. [°C]	45°	45°	45°	45°	40°
	Evaporator Inlet temp. [°C]	45°	45°	42°	47°	40°
	Evaporator Inlet RH [%]	40%	40%	40%	15%	30%
	Condenser Air Flow Rate [m^3 h^{-1}]	2000	2000	2000	2000	1500
	Evaporator Air Flow Rate [kg h^{-1}]	540	540	400	800	550
	Compressor Velocity [rpm]	2750	2750	2750	2750	2400
Other parametres	Humidifier	Unstable	Temporary stability	Small fluctuations	Excluded	Stable
	Air temperature control	Unstable	Unstable	Unstable	Stable	Stable
	Condenser outlet air recirculation	NO	NO	NO	YES	YES
	# TEST	Test 1	Test 2	Test 3	Test 4	Test 5

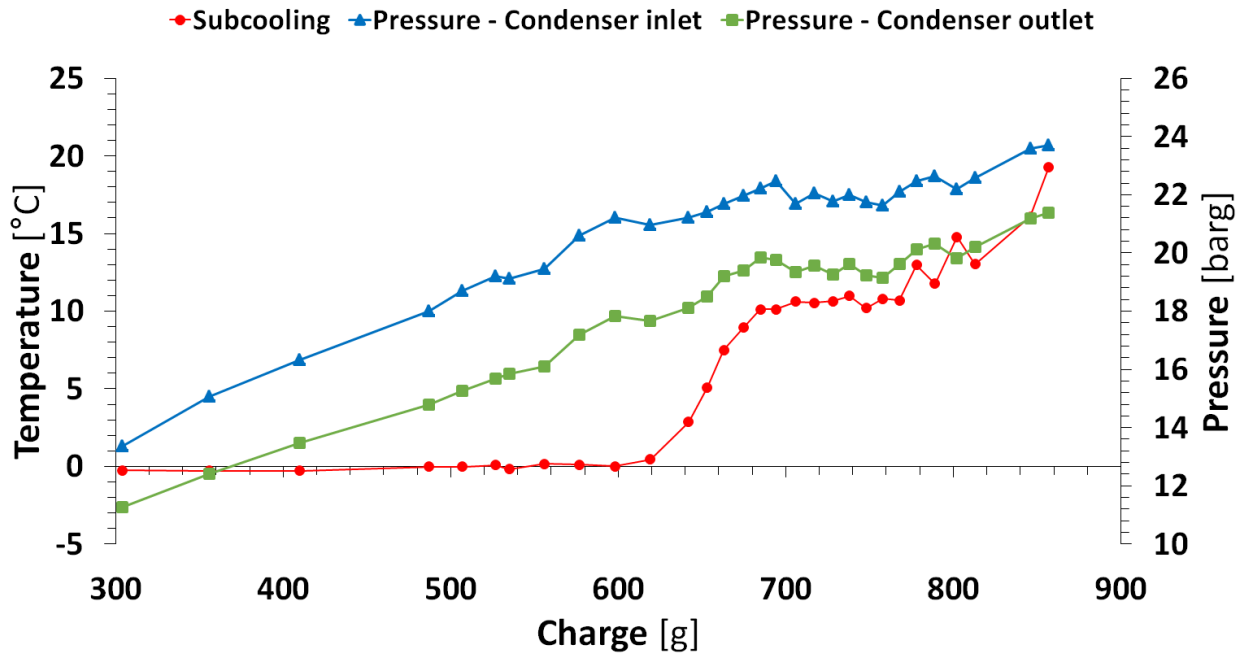Table 1. Set up conditions for the five preliminary tests

Figure 3. Test 1 results: A pronounced instability of the operating plateau is observed
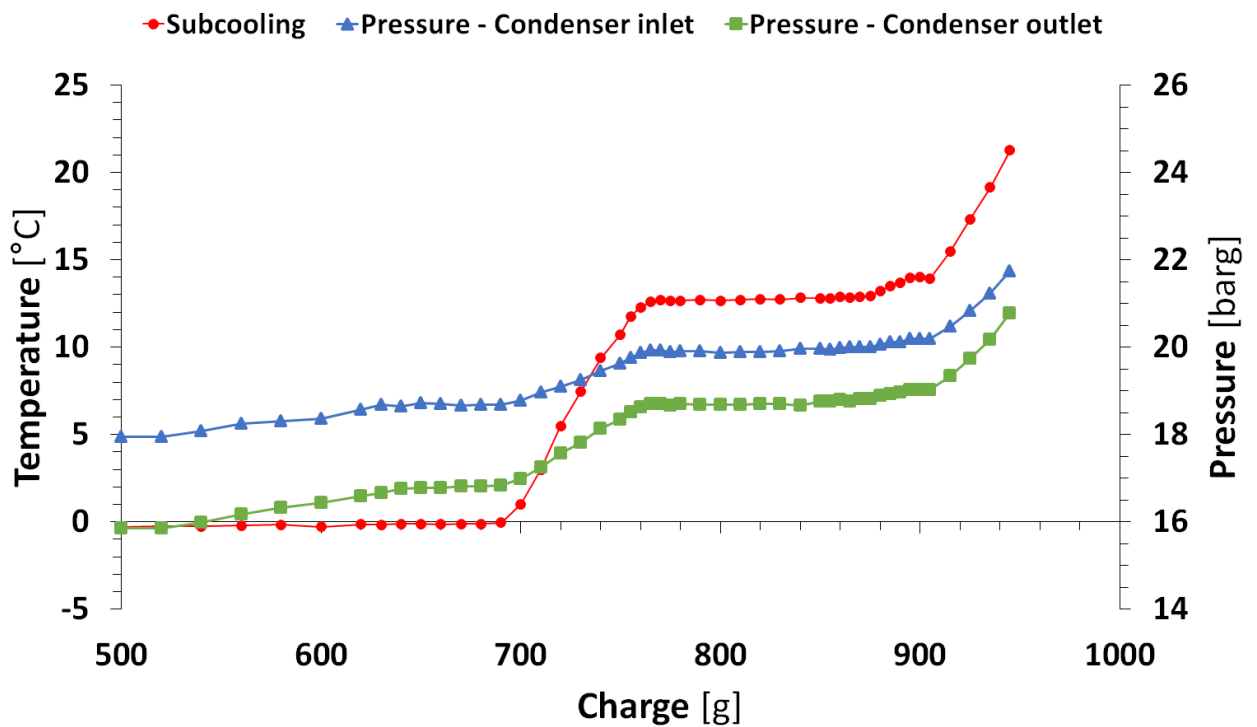

Figure 4. Test 5 results: Stability of operation reached

Figure 3 shows a visible instability of the operating plateau; looking at Table 1, it can be observed how this is due to large instabilities encountered in the humidity and air temperature control. Stability of the temperature inside the condenser wind tunnel could be achieved when recirculation of the air coming out of the condenser was used, as can be seen from test 4 and test 5 results in Table 1.

As shown in Fig. 4, test 5 gives the most stable operating plateau, so its setup has been considered as the reference during the subsequent experimental campaign.

Another test was also carried out, to estimate a proper period of time between two charge steps allowing a sufficient relaxation of the main thermodynamic variables, so that the results are not biased.

The test showed that relaxation of the subcooling value occurs after 3 minutes. Injections of 5g and 10g were compared, and relaxation time proved not to be dependent on this variable.

Finally, influence of the temperatures in the condenser and evaporator wind tunnels was investigated. A test was carried out on a single condenser, and temperatures were varied in the two wind tunnels. Results are shown in Figures 5 and 6; it can be observed how changing the temperatures in the two wind tunnels caused a small variation on the subcooling temperature. However, no significant change in the final plateau length could be observed.
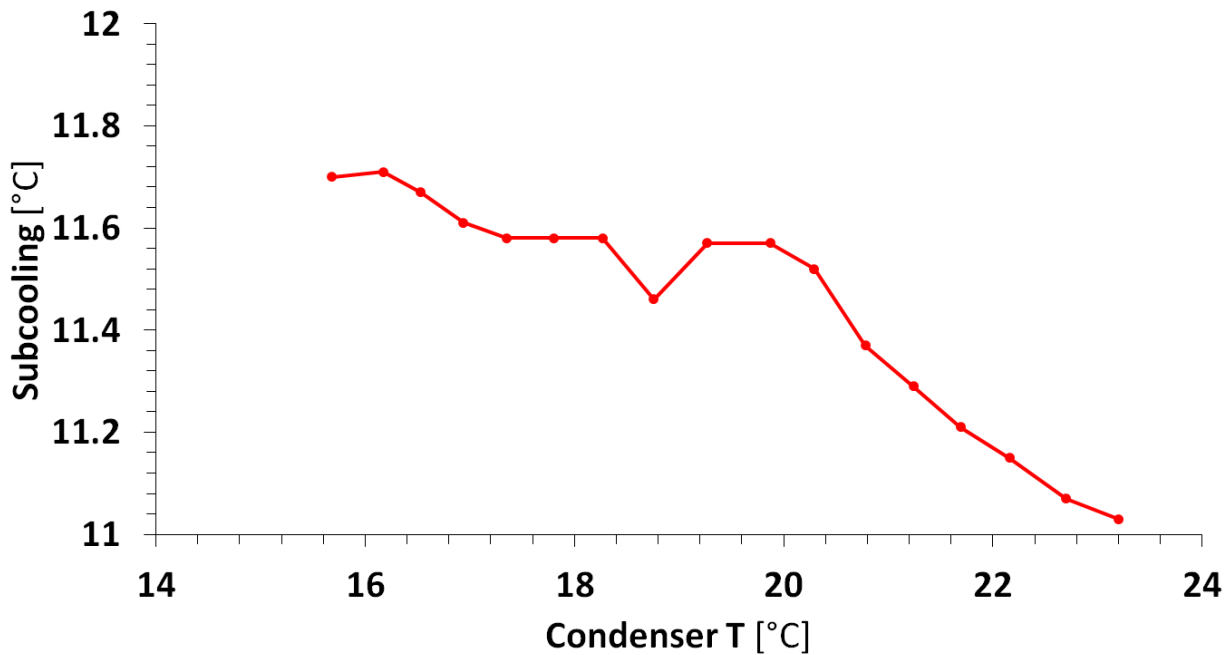

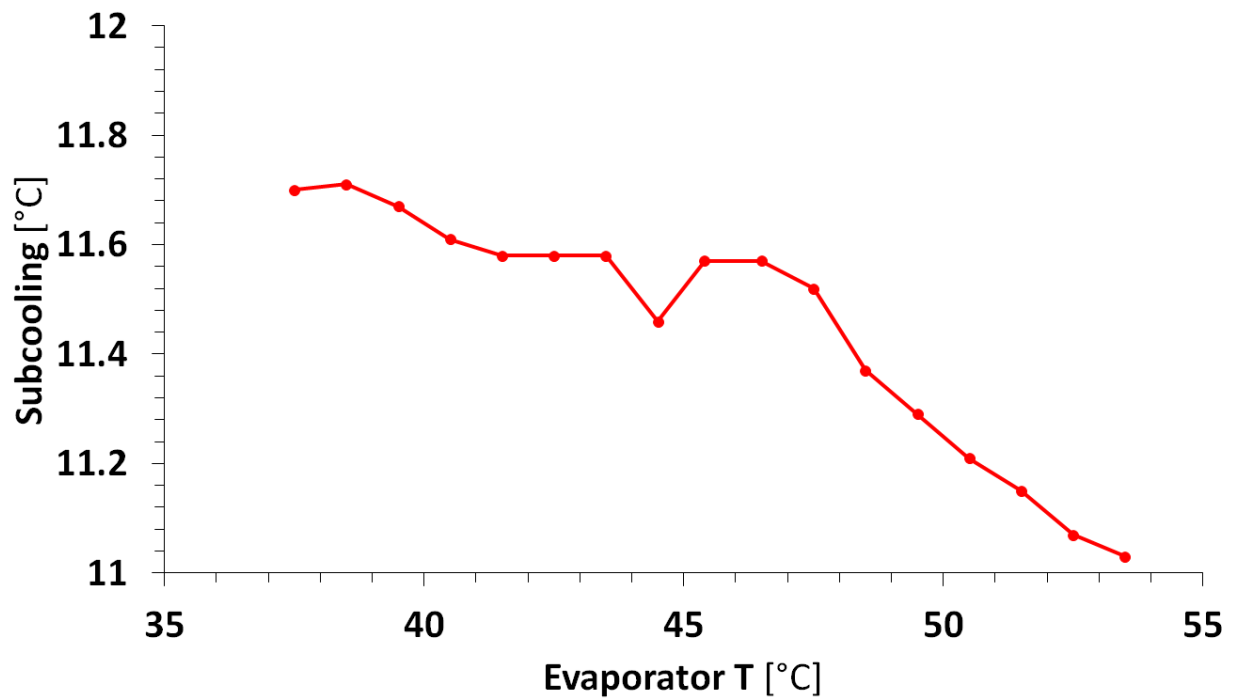Figure 5 Small change in subcooling is osberved when condenser temperature is changed

Figure 6 Small change in subcooling is osberved when evaporator temperature is changed

3. STARTING HYPOTHESIS AND DOE PLANNING

3.1 Receiver filling hypothesis

Preliminary hypothesis on the receiver filling were made considering the results of the preliminary tests; referring to the subcooling curve obtained in test 5, a subdivision of the inner receiver volume is possible.
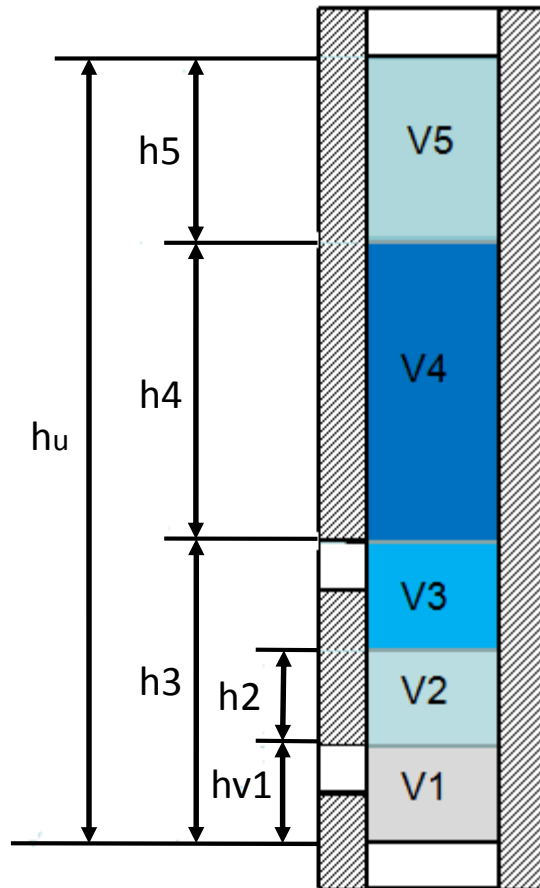
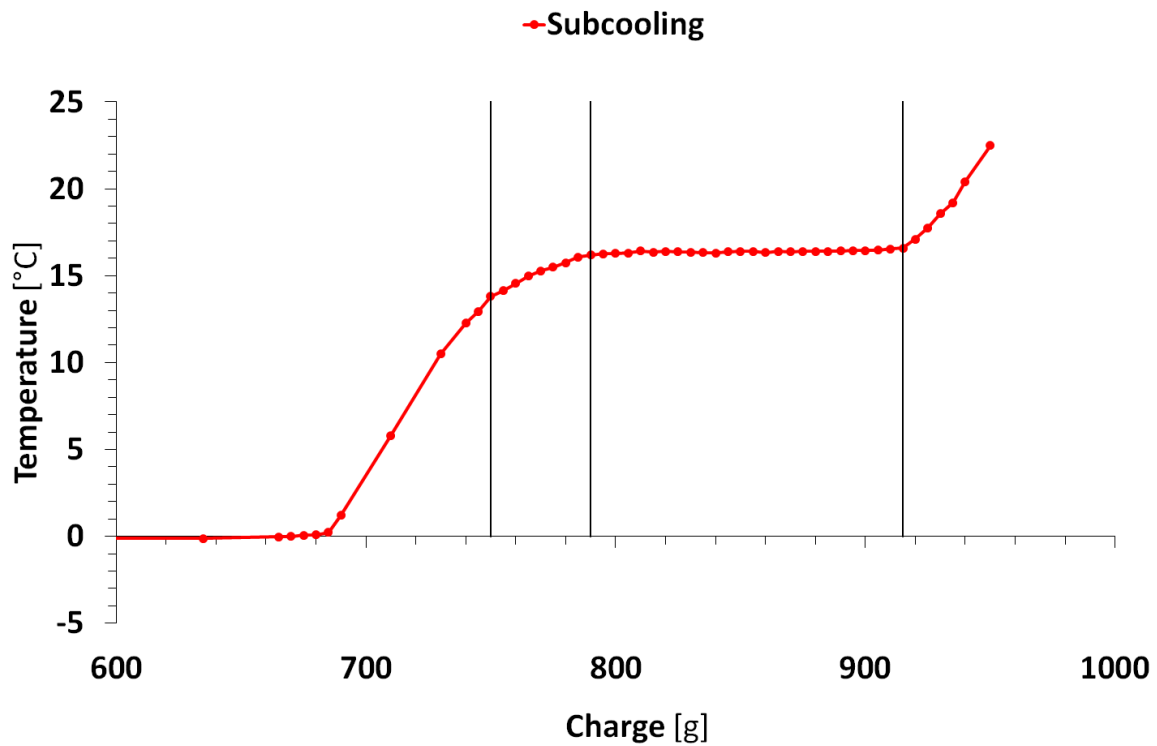Figure 7. Hypothesis of receiver volume subdivision

Figure 8. Subcooling curve with detail on the hypothesized volume separation

By referring to Fig. 7, the volume V1 can be considered as a dead volume, which does not contribute in creating the operating plateau; its existence is hypothesized since it is necessary that the level of liquid in the receiver reaches the outlet in order to have the nominal subcooling value at the condenser exit. The hypothesis is that at least part of this dead volume might correspond, in the curve of Fig. 8, to the area preceding the ramp, meaning that it is filled before a non-zero value of subcooling is observed at the condenser exit.

Volume V2 corresponds to a second dead volume necessary in order to compensate the strong disturbance that the liquid surface encounters during the normal operation of the refrigerant cycle; this extra volume ensures that no gaseous phase enters the last passage of the condenser, so that the nominal subcooling value is reached; on the curve of Fig. 8 this volume might correspond to the "elbow" area where the slope of the ramp gradually reduces, as less and less gaseous phase enters the last passage.

Volumes V3 and V4 form the actual operating plateau; the distinction between the two is only given by the position of the inlet hole, but no difference is expected in the subcooling curve, as shown in Fig. 8.

V5 is the third dead volume hypothesized; its existence could be due to gaseous phase that remains trapped in the upper part of the receiver, preventing the liquid surface to reach the top of the receiver.

These hypothesis are verified with a test using the aforementioned transparent receiver.

3.2 Experimental campaign planning

The factors investigated during the experimental campaign are listed below and were chosen following criteria of importance and easiness of application and modification:

- Inlet and outlet holes position
- Receiver inner diameter
- Receiver height
- Molecular filter presence
- Particle filter presence
- Thermal coupling of the receiver and the condenser header

In order to optimize time and costs, DOE approaches were used in planning the experimental campaign. For the quantitative factors specific domains were set, as described in Table 2. A full factorial design with three factors and two levels was used to investigate holes position and inner diameter of empty receivers, thus excluding filters influence. Prototypes were all manufactured using a fixed inner volume. Hence, as the diameter is changed during the experimental campaign,

also the receiver height varies in order to maintain a constant volume, and can be treated as an implicit factor in the analysis. A second set of experiments was then carried out, according to a fractional factorial design with the same factors and levels as the previous one, but considering receivers filled with both filters, so to allow a comparison with the corresponding empty receivers.

		Levels	
		-	+
	hv1 [mm]	14.3	69.3
Factors	ΔH [mm]	42	130
	diam [mm]	28.9	35.9

Table 2. Domain of investigation

3.3 Results analysis standards

To identify the magnitude of the different volumes described in section 3.1 for all the tests a standard analysis was set, so to have fixed rules to apply during each test.

Volume V1 was calculated considering only the distance of the upper edge of the outlet hole from the receiver base.

The magnitude of the operating plateau and the corresponding volumes V3 and V4 were identified taking into consideration all the points included within a 0.5 °C wide band along the subcooling axis (see Fig. 9).
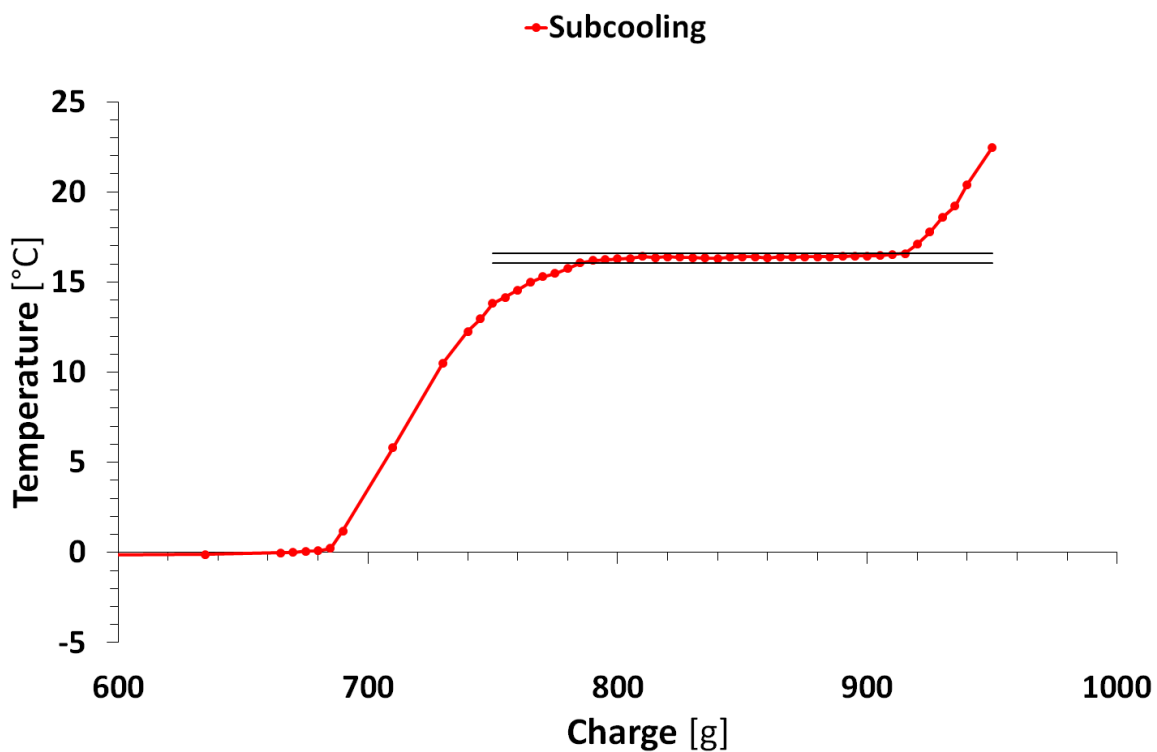

Figure 9. Rule for plateau magnitude determination

Finally, V2 and V5 were determined as a difference between the receiver inner volume and the other volumes already calculated and measured.

As mentioned above, these volumes were used to build a function able to evaluate the filling efficiency of the receiver. In this paper, the expression of this efficiency is given by:

$$\varepsilon = \frac{V_{plateau}}{V_{useful}} = \frac{V3 + V4}{V_{useful}} = 1 - \frac{V1 + V2 + V5}{V_{useful}}$$

(1)

Clearly, this formula can be conveniently recast in terms of the heights only, as follows:

$$\varepsilon = 1 - \frac{h1 + h2 + h5}{h_{useful}}$$

(2)

where again $h1$ and h_{useful} are geometrical parameters.

4. TRANSPARENT RECEIVER TEST RESULTS

Before running the experimental campaign, a test on a transparent receiver was carried out in order to assess the existence of the hypothesized volumes. For this test, different operative conditions with respect to the reference set up were used, because of safety issues due to poorer resistance to stresses of the polycarbonate used for manufacturing the receiver.
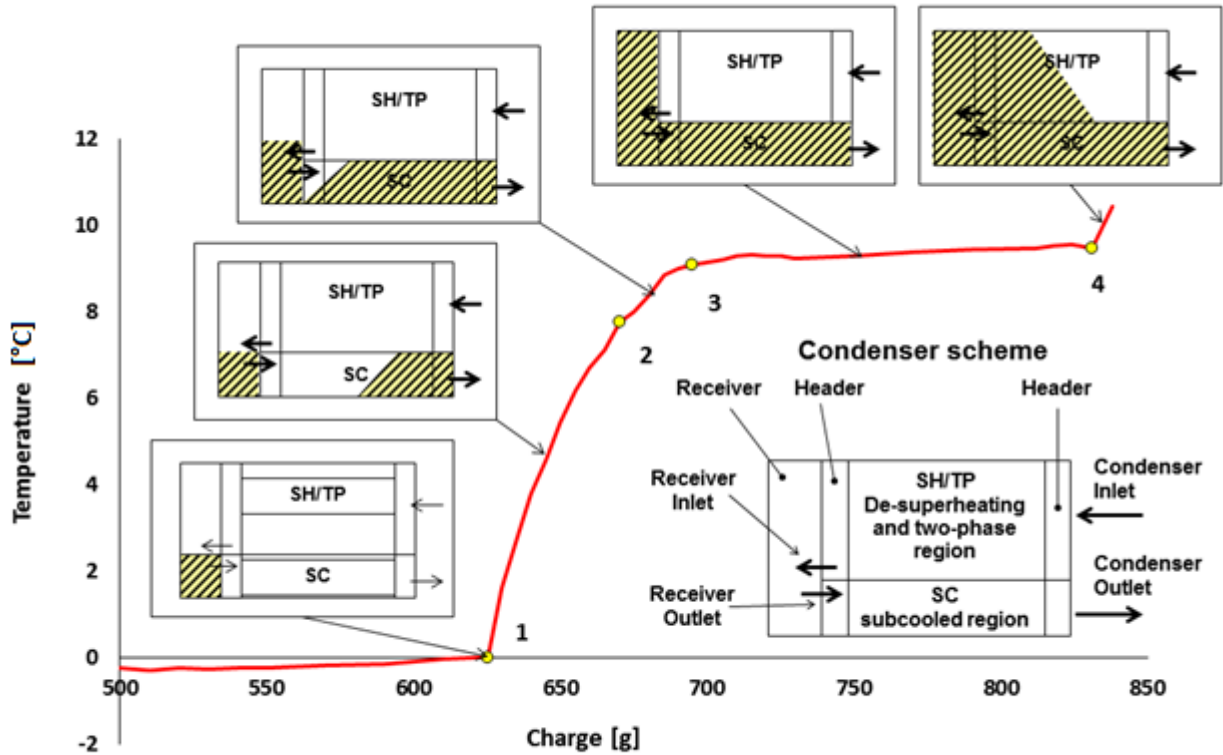
Figure 10. Transparent receiver - test results highlighting the phases of the receiver filling

The test showed a stable operating plateau, meaning that the use of a different material for the receiver construction did not cause any substantial change in the filling process (Fig. 10).
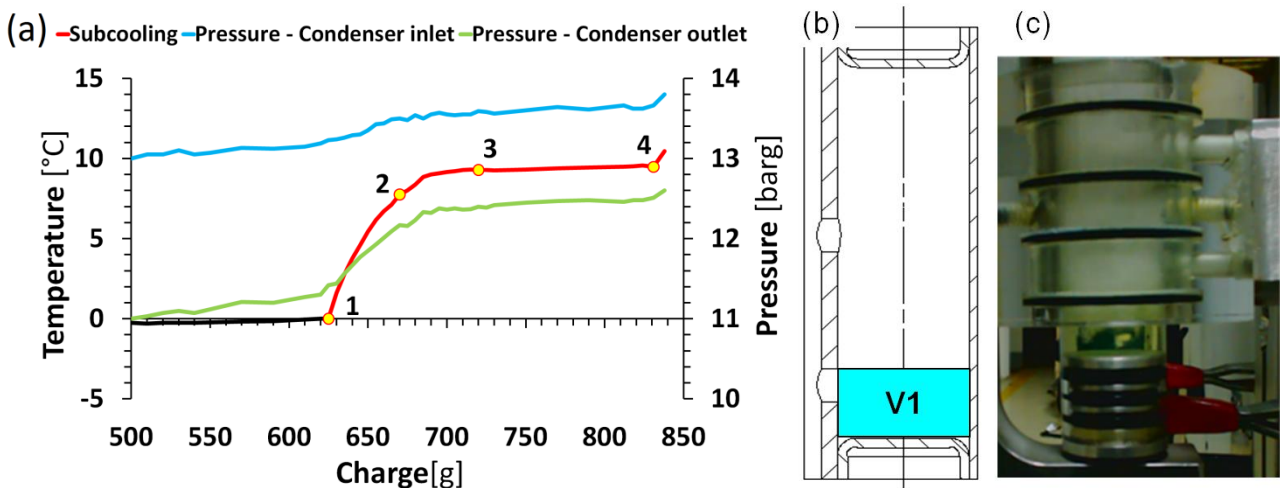

Figure 11. Before-ramp phase, before point 1 in Fig. 8: (a) thermodynamic quantities; (b) filled volume in the receiver schematic and (c) experimental picture of the transparent receiver in the representative state

Analysis of the test footage led to some important conclusions:

- Before reaching a non-zero value of subcooling at the condenser outlet, i.e. before ramp phase (see Fig. 11), the part of receiver under the upper edge of lower hole is being

filled (volume V1 in Fig. 11(b)), as confirmed in Fig. 11(c). Note that, at point 1, only the lower part of the receiver is filled of liquid refrigerant, while, in the rest of the condenser, refrigerant is either in the gas or two-phase state. Moreover, as visible in Fig. 11(c), the strong turbulence experienced in the experiment prevented to assess if the liquid surface reaches the upper edge of the hole, or if the remaining part is filled during the subsequent phase (i.e. the ramp phase).
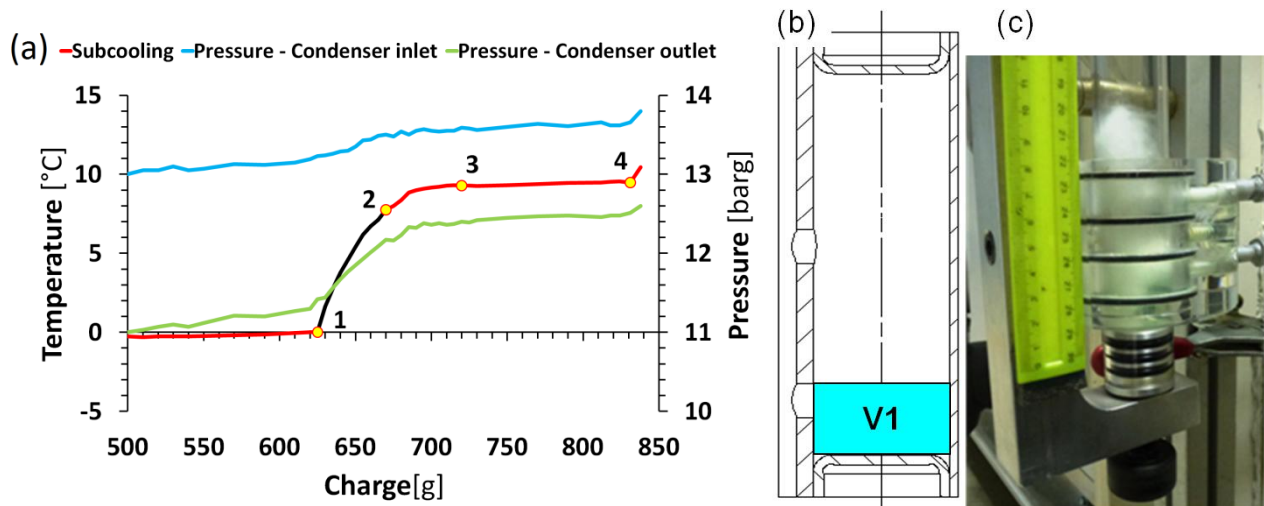

Figure 12. Ramp phase, line 1-2 in Fig. 8: (a) thermodynamic quantities; (b) filled volume in the receiver schematic and (c) experimental picture of the transparent receiver in the representative state

- Although a strong change in the subcooling values is observed during the ramp phase (see Fig. 12(a)), no significant change is visible in the receiver (see Fig. 12(b-c)). This is because flooding of the last passage of the condenser is occurring in this phase: Hence any further increase in the charge goes directly in the condenser and is not stored in the receiver. This supports the conclusion that the volume V1 at this point is completely filled and obviously does not give contribution to the operating plateau (see Fig. 12(b)).
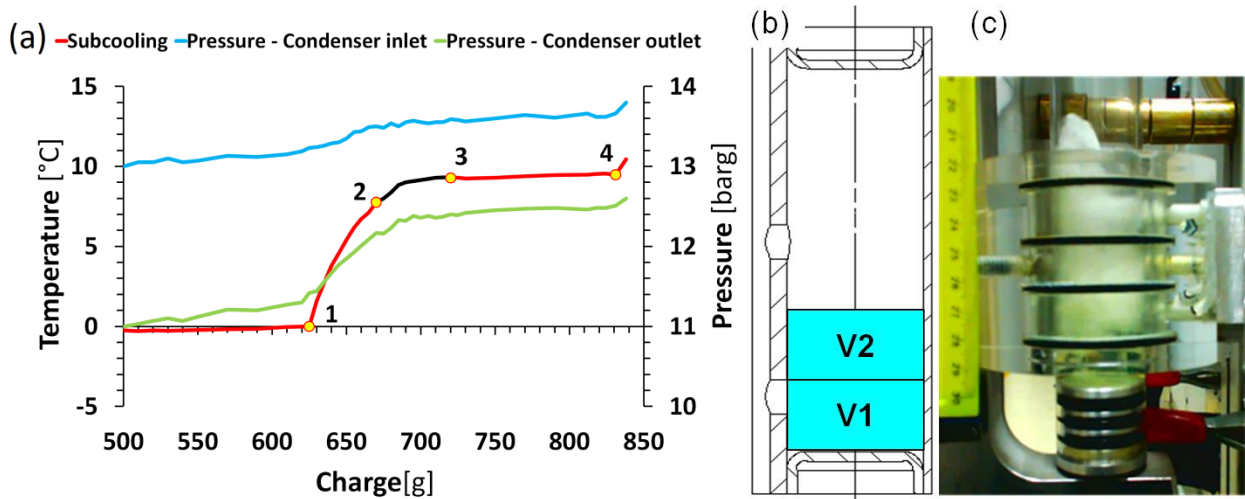
Figure 13. Elbow phase, line 2-3 in Fig. 8: (a) thermodynamic quantities; (b) filled volume in the receiver schematic and (c) experimental picture of the transparent receiver in the representative state

- After the injection of a certain amount of refrigerant, the ramp phase ends and the level of the liquid surface in the receiver starts rising again (see Fig. 13(b-c)). This phase corresponds to a transition stage in which flooding of the last passage of the condenser is about to be completed, but part of the injected refrigerant is now being stored in the receiver, thus reducing the slope of the ramp progressively (see Fig. 13(a)). For this reason, we identify an additional volume that gives no contribution to the operating plateau. This volume is called V2 and is due to vapour bubbles that flow downwards to the outlet hole.
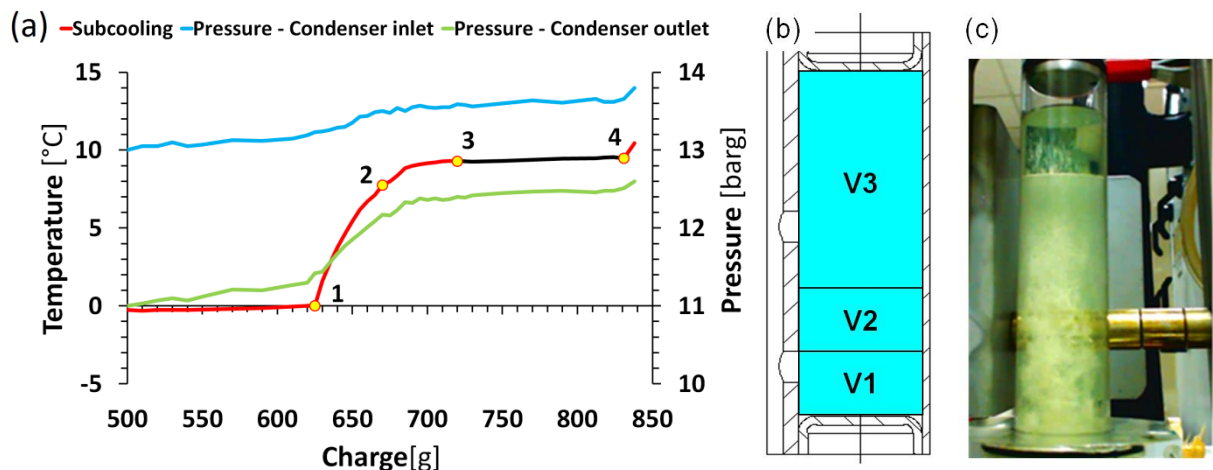

Figure 14. Plateau phase, line 3-4 in Fig. 8: (a) thermodynamic quantities; (b) filled volume in the receiver schematic and (c) experimental picture of the transparent receiver, which shows the receiver flooding

- When the operating plateau starts forming (see Fig. 14(a)), turbulence is strongly reduced and the liquid surface becomes visible (see Fig. 14(c)): all refrigerant injected is

now stored in the receiver. The receiver filling (and consequently the plateau formation) continues until the top of the receiver is reached (point 4 in Fig. 10). Note that, despite the fact that the receiver is completely filled of liquid refrigerant, only a part of this liquid contributes to plateau (volume V3 in Fig. 14(b)). In Fig. 14(b), former volumes V3, V4 and V5 (see Fig. 7) were merged for the sake of simplicity (V5 is actually zero, see next).
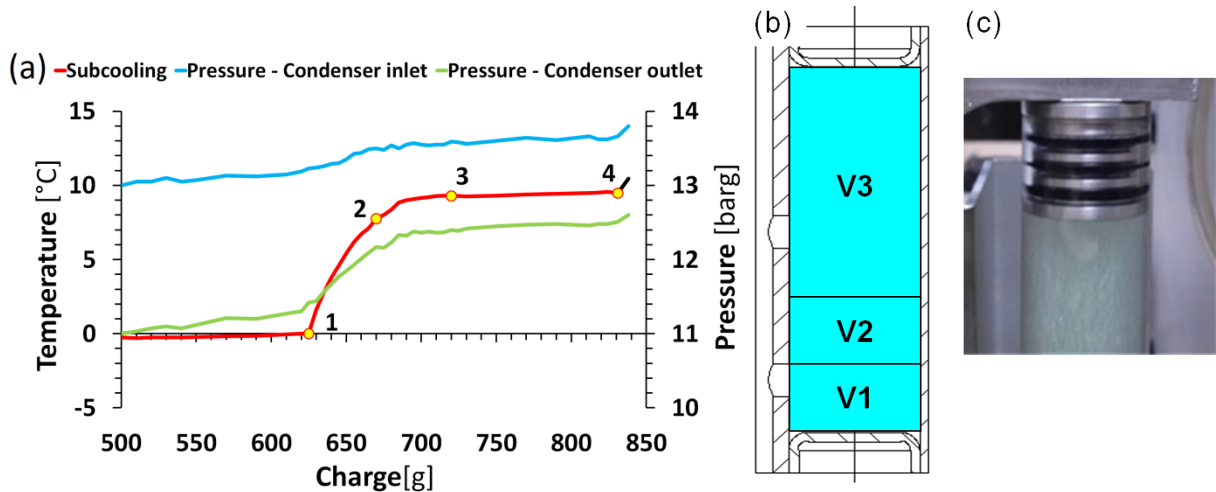

Figure 15. After-plateau phase, beyond point 4 in Fig. 8: (a) thermodynamic quantities; (b) filled volume in the receiver schematic and (c) experimental picture of the transparent receiver, which is completely filled

- After the receiver is completely filled (see Fig. 15(c)), if the charge continues, then the condenser will be flooded. Consequently condenser pressure and subcooling will increase, but no change will occur inside the receiver.

Taking into account the complete filling of the receiver (see Fig. 15(c)), the efficiency formula proposed above can be modified by neglecting the volume V5, namely

$$\varepsilon = 1 - \frac{h1 + h2}{h_{useful}}$$

(3)

$$\varepsilon = 1 - \frac{h1 + h2}{h_{useful}}$$

5. TESTS RESULTS

5.1 Empty receivers

After having characterized the different phases of the filling process and found a suitable subdivision of the receiver useful volume, the actual experimental campaign was started.

As mentioned in section 3.2 the experimental campaign firstly focused on empty receivers, thus not including the molecular and particle filters. DOE techniques were used to investigate the main effects of:

- the holes position, in terms of height of the outlet hole hv1 and holes axle spacing ΔH;

- the inner diameter;

- the mutual interactions between the above parameters.

Prototype	hv1	ΔH	diam	hv1 x ΔH	hv1 x diam	ΔH x diam	h2 [mm]	Efficiency [%]
1	-	-	+	+	-	-	67.7	56.3%
2	-	+	-	-	+	-	105.3	56.3%
3	+	-	-	-	-	+	74.3	58.5%
4	+	+	+	+	+	+	87.8	39.3%
5	-	-	-	+	+	+	75.0	64.9%
6	-	+	+	-	-	+	93.2	39.4%
7	+	-	+	-	+	-	58.5	45.0%
8	+	+	-	+	-	-	103.8	47.8%

Table 3. Full factorial DOE for geometrical factors investigation

Following the scheme in Table 3, for each of the eight tests carried out, we measured the values of h2 (necessary for the model construction) and the filling efficiency (necessary to make the final comparison between estimated and measured efficiency). These results were then analyzed in order to evaluate the magnitude of the three main effects and their interactions. Results in Table 4 show that the axle spacing between holes and the inner diameter have the strongest influence on h2. In particular, an increase in the axle spacing caused a remarkable increase in h2 and, consequently, a decrease of efficiency. An increase of the inner diameter causes a reduction of h2, but the combined effect of the two still produces a reduction in the filling efficiency.

	Plateau length [g]	Efficiency [%]
hv1 effect	-10	-6.6%
ΔH effect	-17.5	-10.4%
diam effect	-22.5	-11.9%
hv1 x ΔH	2.5	2.3%
hv1 x diam	2.5	0.9%
ΔH x diam	0	-0.8%

Table 4. Factors' influence magnitude

Other factors are found to have a secondary influence.

Some other tests were carried out in addition to the one of the DOE, in order to collect more data to be used at a later time for the model construction, and they all gave results in accordance to the trends already found.

The fourth factor investigated was how much adiabatic the receiver is: Because of the thermal contact with the condenser manifold, the latter condition coincides with how much isothermal the receiver can be assumed, with regards to the condenser. The two-passage condensers are naturally at the same temperature of the receiver and hence the latter can be considered as adiabatic. For more than two passages, a temperature difference exists between the condenser and the receiver and hence the receiver cannot be assumed as adiabatic anymore. In the fitting model, the receiver is always assumed as adiabatic, even in the case of four-passage receivers. Hence, in the latter case, model discrepancies may be due also to thermal fluxes through the receiver walls.
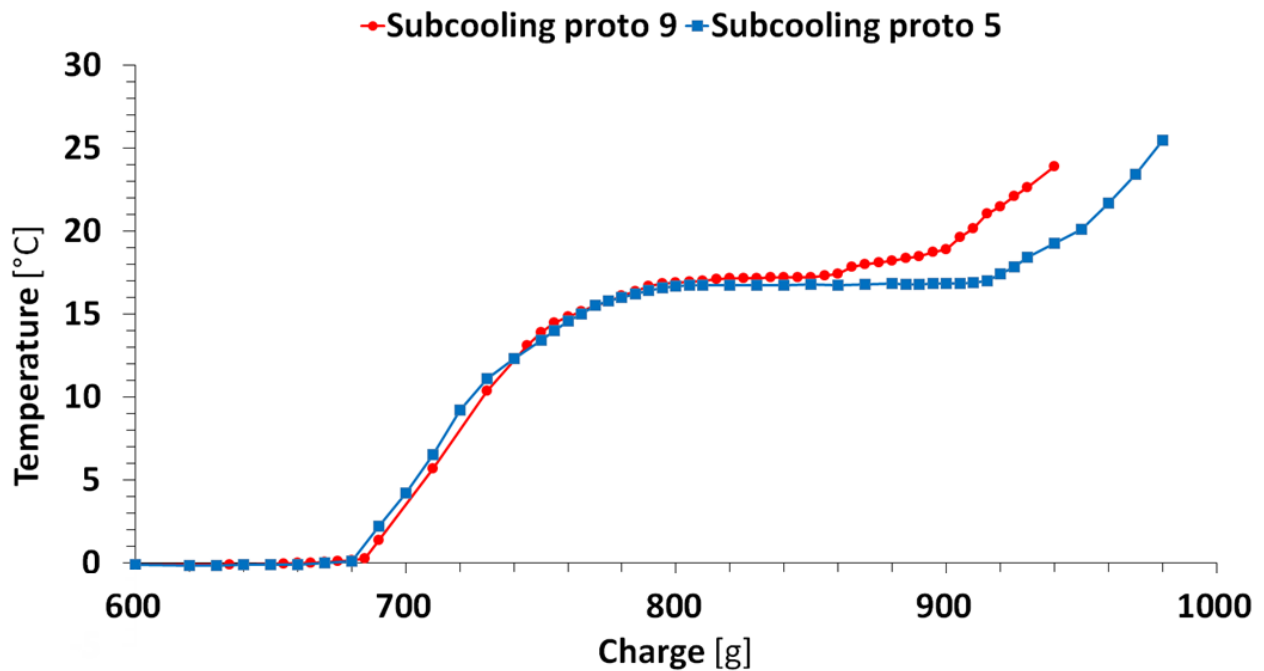

Figure 16. Effect of number of passages on plateau magnitude: Proto 9 with 4 passages, Proto 5 with two passages

As can be seen in Fig. 16, the four-passage condenser curve (proto 9) shows an early slope change in the subcooling curve, which is not present in the two-passage case (proto 5). This obviously causes a worsening on the receiver operation and so on the condenser performance.

A more accurate analysis of the region where those slope changes occur led to the conclusion that they are caused by heat transfer between the receiver and the condenser, because the latter parts are not isothermal in case of condensers with more than two passages.
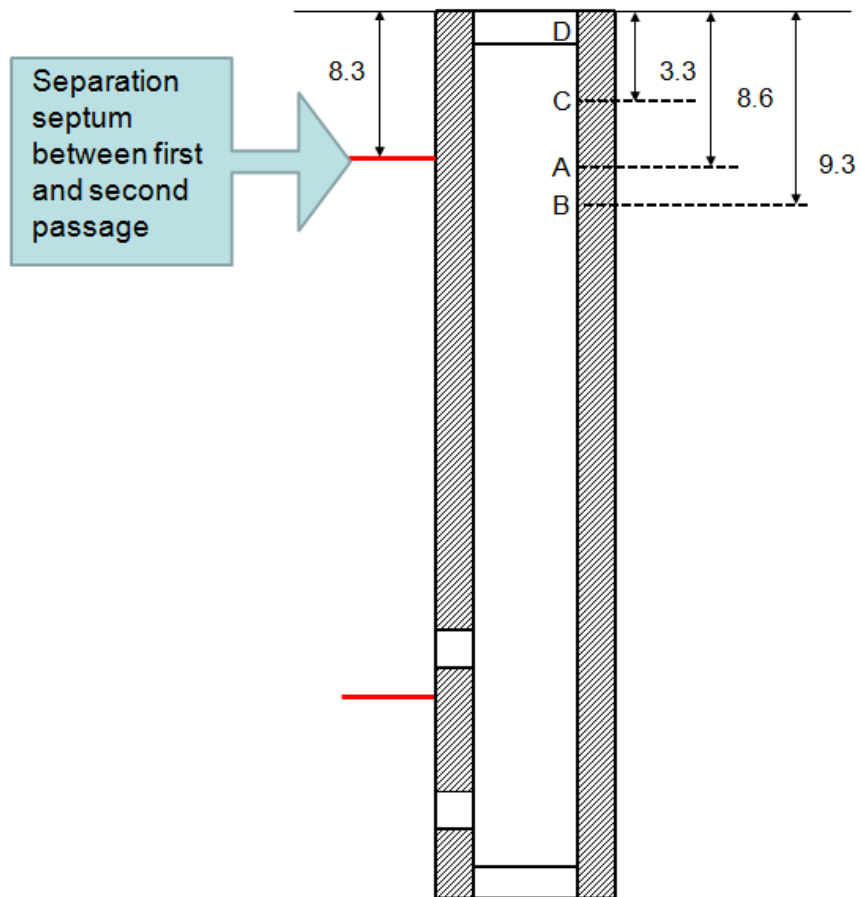
Figure 17. Analysis on condenser circuitation effect

As showed in Fig. 17, it was calculated that the first point of slope change in the "proto 9" curve of Fig. 18 corresponds to the point in the manifold where a septum, separating two passages, is placed (points A-B): the two passages separated by the septum carry refrigerant with very different temperature, the upper being hotter than the lower which has undergone one more passage in the condenser, thus creating the mentioned different heat transfer conditions. This example explains why the condenser and the receiver are not isothermal in case of more than two passages.

As a confirmation, another four-passage condenser was tested, named "proto 10", using the same receiver as the previous two, but this time an axle spacing between receiver and manifold was created by milling; Fig. 16 shows that now the early slope change does not occur and the condenser behaves the same way as its two-passage homologous.
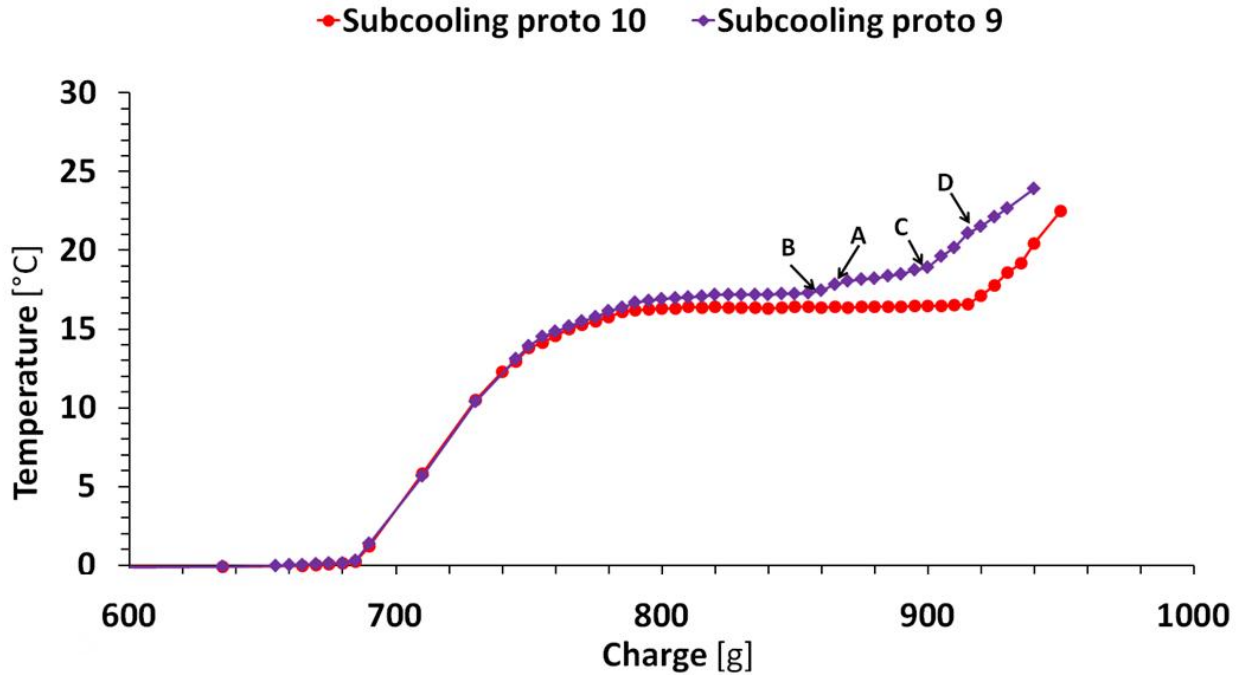
Figure 18. Identification of the points A-D of figure 15 on the subcooling curve: the slope change occurring in point A-B of proto 9 curve is no more present in the proto 10 curve, after insulating the receiver.

Thickness of the receiver wall may influence the entity of the heat flux exchanged; this parameter was not investigated though because it was believed that insulation of the receiver through the creation of the axle spacing would have sufficed to bring the plateau length to a normal value. The improvement obtained through this procedure was considered sufficient so no further analysis of the problem was carried out.

5.2 Receivers with filters

The last two factors analyzed concern the filters insertion and how they affect the receiver filling. This investigation was carried out with a fractional factorial DOE taken from the full factorial used before, so to compare the results of the same receiver in both the empty configuration and then the one filled with the two filters (Table 5).

Proto	hv1	ΔH	Diam	Δg plateau [g]
1f	-	-	+	30
2f	-	+	-	25
3f	+	-	-	20
4f	+	+	+	25

Table 5. Fractional factorial DOE for filter effect investigation

	Δg plateau [g]
hv1 effect	-5
ΔH effect	0
diam effect	5

**Table 6. Effects of the geometrical factors
on the plateau magnitude reduction**

In this analysis only the modification on the plateau magnitude was taken into account.

As shown in Table 5, the difference in the plateau magnitude is around 25 g of refrigerant corresponding to about 25 cm^3 (under the considered operating conditions, the density of the refrigerant is roughly 1 g cm^{-3}), which amounts to the volume occupied by the molecular filter. Recalling that the refrigerant injection precision is 5 g, it was concluded that the analysis of the main effects of three geometrical factors under study did not produce evidence of any particular effect on the plateau magnitude change other than the simple reduction due to the filter volume itself (Table 6).

About the particle filter, a specific test carried out using only this filter and not both of them made clear that its effect can be considered negligible, likely due to its position and small volume (about 5cm^3), even though the small volume of the particle filter is taken into account in the computation of the net volume for the charge (see next section).

6. FILLING EFFICIENCY CORRELATION

6.1 Empty receivers

Results from the various tests described above were finally put together to build up a model able to estimate the filling efficiency. As a first step, a model for empty receivers was constructed, using the three geometrical parameters described before, and assuming that the condenser is either of the two-passage type, or a four-passage thermally insulated condenser, which satisfies the isothermal assumption between the condenser and the receiver, as discussed in section 5.1.

Looking at the efficiency formula reported at the end of section 4, it is clear that, given hv1 and h_{useful} as geometric inputs, the only variable for a given receiver is h2. As a consequence, for the efficiency calculation a model that estimates h2 is necessary.

To this end, it was decided to build a model which uses the least number of coefficients, yielding however a sufficient level of accuracy; this was done in order to guarantee a certain model flexibility, so that it may be applied for a larger group of receivers. For this reason, squared terms were considered negligible and excluded from model from the beginning. Concerning mutual interaction terms, different solutions were investigated, using different combinations of the interaction terms of the three considered variables, starting from the complete expression:

$$\frac{h2}{h2_0} = c_1 * \frac{hv1}{hv1_0} + c_2 * \frac{\Delta H}{\Delta H_0} + c_3 * \frac{D}{D_0} + c_4 * \frac{hv1}{hv1_0} * \frac{\Delta H}{\Delta H_0} + c_5 * \frac{hv1}{hv1_0} * \frac{D}{D_0} + c_6 * \frac{\Delta H}{\Delta H_0} * \frac{D}{D_0}$$

(4)

$$\frac{h2}{h2_0} = c_1 \left(\frac{hv1}{hv1_0}\right) + c_2 \left(\frac{\Delta H}{\Delta H_0}\right) + c_3 \left(\frac{D}{D_0}\right) + c_4 \left(\frac{hv1}{hv1_0}\right)\left(\frac{\Delta H}{\Delta H_0}\right) + c_5 \left(\frac{hv1}{hv1_0}\right)\left(\frac{D}{D_0}\right) + c_6 \left(\frac{\Delta H}{\Delta H_0}\right)\left(\frac{D}{D_0}\right)$$

Model	Max error on ε
Linear	17.6%
hv1 x D	16.1%
hv1 x D + hv1 x ΔH	15.3%
ΔH x D	4.6%
hv1 x D + ΔH x D	3.9%
hv1 x ΔH + ΔH x D	4.7%
Complete	3.7%

Table 7. Models accuracy comparison

The subscript 'o' indicates reference quantities used for normalization purposes.

As shown in Table 7, models that include the coefficient of the interaction between holes axle spacing and inner diameter (ΔH x D) gave the best results in terms of the accuracy in predicting h2 and the filling efficiency. Among this subgroup, the model with fewer coefficients was chosen.

$$\frac{h2}{h2_0} = c_1 * \frac{hv1}{hv1_0} + c_2 * \frac{\Delta H}{\Delta H_0} + c_3 * \frac{D}{D_0} + c_4 * \frac{\Delta H}{\Delta H_0} * \frac{D}{D_0}$$

(5)

$$\frac{h2}{h2_0} = c_1 \left(\frac{hv1}{hv1_0}\right) + c_2 \left(\frac{\Delta H}{\Delta H_0}\right) + c_3 \left(\frac{D}{D_0}\right) + c_4 \left(\frac{\Delta H}{\Delta H_0}\right)\left(\frac{D}{D_0}\right)$$

C1/C2	-2.1 %
C2/C2 (main)	100.0 %
C3/C2	11.0 %

C4/C2	-70.4 %

Table 8. Normalized model coefficients

From the analysis of the coefficients in Table 8, it can be concluded that reducing the inner diameter and the holes axle spacing produces a great reduction of h2 and consequently an increase of the filling efficiency. Reducing the distance of the outlet hole from the receiver bottom also produces an h2 decrease, but its effect is at least one order of magnitude weaker than the previous two.

6.2 Receivers with filter

To account for the filters presence, a modification of the existing model was implemented, following two different approaches: i) modification of the useful value, reducing it of a quantity corresponding to the dummy height calculated from the filters volume (method " Hus' "); ii) new h2 model using measurements of h2 obtained considering the apparent base area, calculated taking into account the filter encumbrance (method "New H2"). The first approach was preferred, because in this way the model can be still applied even if the size or type of the filters is changed; the same would not be possible if a model of h2 was built using only the results of the receiver tested with the present filters.

Prototype	Errors on ε	
	Method Hus'	Method New H2
1f	1.3%	0.8%
2f	3.6%	8.2%
3f	5.6%	4.7%
4f	0.1%	1.9%
11f	6.9%	8.6%
12f	1.7%	5.3%

Table 9. Model accuracy of the two solutions for the filter insertion

Table 9 shows that this modification causes a slight worsening of the model accuracy, which is still sufficient for industrial applications.

The complete model will finally use the h2 formula given previously in the revised efficiency expression, where the useful height has been reduced for taking into account the presence of the filter, namely

$$\varepsilon = 1 - \frac{hv1 + h2}{h_{useful}}$$

(6)

$$\varepsilon = 1 - \frac{hv1 + h2}{h_{useful}}$$

7. CONCLUSIONS

In this paper a detailed analysis of the behaviour of the integrated receiver in automotive condensers has been carried out. Different prototypes were tested in a test bench able to reproduce boundary conditions similar to the in-vehicle tests. A starting hypothesis on the receiver volume usage was verified with a test on a transparent receiver, which demonstrated the existence of two dead volumes that give no contribution to the operating plateau formation; a third dead volume was instead proven to be negligible. It was also demonstrated that, in case of four-passage condensers, thermal insulation of the receiver is necessary, in order to ensure the creation of a longer stable plateau; for two-passage condensers, the receiver can be naturally assumed as adiabatic.

A model to estimate the filling efficiency of adiabatic receivers has then been obtained; the analysis on the coefficient suggests that minimization of inner diameter and holes axle spacing is a good practice in order to enhance the performance of the receiver and produce refrigerant saving. The correction of the model that takes into account the filter presence slightly worsens the accuracy, which is however still sufficient for industrial application.

REFERENCES

[1] R.K. Shah, ''Automotive air-conditioning systems – historical developments, the state of technology and future trends'', *Proceedings of the 3rd BSME-ASME International Conference on Thermal Engineering,* Dhaka (Bangladesh), December 20-22, 2006

[2] M. Ferrero, A. Scattina, E. Chiavazzo, F. Carena, D. Perocchio, M. Roberti, G. Toscano Rivalta, P. Asinari, "Louver Finned Heat Exchangers for Automotive Sector: Numerical Simulations of Heat Transfer and Flow Resistance Coping With Industrial Constraints", *Journal of Heat Transfer*, 135, 121801, 2013

[3] J. Jang, C. Cheng, "Optimization of the louver angle and louver pitch for a louver finned and tube heat exchanger", *International Journal of Physical Sciences,* 8:43, pp. 2011-2022, 2013

[4] Y. Yamanaka, H. Matsuo, K. Tuzuki, T. Tsuboko, Y. Nishimura, "Development of sub-cool system"*, Society of Automotive Engineers (SAE),* doi:10.4271/970110, 1997

[5] Von Roland Burk, "Kondensatormodul fur Kraftfahrzeug-Klimaanlagen", *ATZ Automobiltechnische Zeitschrift,* 97:5, 1995

[6] V. Pomme, " Improved automotive A/C systems using a new forced subcooling technique", SAE Technical Papers, DOI: 10.4271/1999-01-1192, 1999.

[7] Z. Qi, Yu Zhao, J. Chen, "Performance enhancement study of mobile air conditioning system using microchannel heat exchangers", *International Journal of Refrigeration*, 33:2, pp. 301–312, 2010

[8] B. A. Qureshi, S. M. Zubair, "Mechanical sub-cooling vapor compression systems: Current status and future directions", *International Journal of Refrigeration,* 36:8, pp. 2097–2110, 2013

[9] J. Khan, S. M. Zubair, "Design and rating of an integrated mechanical-subcooling vapor-compression refrigeration system", *Energy Conversion & Management,* 41:11, pp. 1201–1222, 2000

[10] G. H. Lee, J. Y. Yoo, "Performance analysis and simulation of automobile air conditioning system", *International Journal of Refrigeration*, 23:3, pp. 243–254, 2000

[11] N. Vjacheslav, A. Rozhenstev, C. Wang, "Rationally based model for evaluating the optimal refrigerant mass charge in refrigerating machines", *Energy Conversion and Management,* 42:18, pp. 2083–2095, 2001

[12] V. Pomme, "Improved automotive A/C system using a new forced subcooling technique", *Valeo Climate,* 1999

[13] J. B. Jensen, S. Skogestad, "Optimal operation of simple refrigeration cycles Part I: Degrees of freedom and optimality of sub-cooling", *Computers and Chemical Engineering,* 31:5–6, pp. 712–721, 2007

[14] J. P. Koeln, A. G. Alleyne, "Optimal subcooling in vapor compression systems via extremum seeking control: Theory and experiments", *International Journal of Refrigeration,* 43, pp. 14–25, 2014

[15] M. Parrino, M. Dongiovanni, M. Milone, M. Chiara, "Influence of receiver capacity on the refrigerant charge and on the performance of an A/C system", *Society of Automotive Engineers (SAE)*, doi:10.4271/1999-01-0871, 1999

[16] K. Prolss, G. Schmitz, D. Limperich, M. Braun, "Influence of Refrigerant Charge Variation on the Performance of an Automotive Refrigeration System", *International Refrigeration and Air Conditioning Conference,* Purdue, July 17-20, 2006

[17] N. C. Strupp, J. Kholer, N. C. Lemke, W. Tegethoff, R. M. Kossel, "Energy efficient future automotive condenser systems", *International Symposium on Next-generation Air Conditioning and Refrigeration Technology,*Tokyo (Japan), February 17–19, 2010

[18] G. Pottker, P. Hrnjak, "Effect of Condenser Subcooling of the Performance of Vapor Compression Systems: Experimental and Numerical Investigation", *International Refrigeration and Air Conditioning Conference,* Purdue, July 16-19, 2012

LIST OF TABLES

LIST OF FIGURES

Figure 10. Transparent receiver - test results highlighting the phases of the receiver filling

Figure 11. Before-ramp phase, before point 1 in Fig. 8: (a) thermodynamic quantities; (b) filled volume in the receiver schematic and (c) experimental picture of the transparent receiver in the representative state

Figure 12. Ramp phase, line 1-2 in Fig. 8: (a) thermodynamic quantities; (b) filled volume in the receiver schematic and (c) experimental picture of the transparent receiver in the representative state

Figure 13. Elbow phase, line 2-3 in Fig. 8: (a) thermodynamic quantities; (b) filled volume in the receiver schematic and (c) experimental picture of the transparent receiver in the representative state

Figure 14. Plateau phase, line 3-4 in Fig. 8: (a) thermodynamic quantities; (b) filled volume in the receiver schematic and (c) experimental picture of the transparent receiver, which shows the receiver flooding

Figure 15. After-plateau phase, beyond point 4 in Fig. 8: (a) thermodynamic quantities; (b) filled volume in the receiver schematic and (c) experimental picture of the transparent receiver, which is completely filled

Figure 16. Effect of number of passages on plateau magnitude: Proto 9 with 4 passages, Proto 5 with two passages

Figure 17. Analysis on condenser circuitation effect

Figure 18. Identification of the points A-D of figure 15 on the subcooling curve: the slope change occurring in point A-B of proto 9 curve is no more present in the proto 10 curve, after insulating the receiver.